Cancer Cell
Article

Oncogene-Targeting T Cells Reject Large Tumors while Oncogene Inactivation Selects Escape Variants in Mouse Models of Cancer

Kathleen Anders,[1] Christian Buschow,[2] Andreas Herrmann,[4] Ana Milojkovic,[5] Christoph Loddenkemper,[3] Thomas Kammertoens,[2] Peter Daniel,[5] Hua Yu,[4] Jehad Charo,[1] and Thomas Blankenstein[1,2,*]
[1]Max-Delbrück-Center for Molecular Medicine, 13092 Berlin, Germany
[2]Institute of Immunology
[3]Institute of Pathology
Charité Campus Benjamin Franklin, 12200, Berlin, Germany
[4]Cancer Immunotherapeutics and Tumor Immunology, Beckman Research Institute, City of Hope Cancer Center, Duarte, CA 91010, USA
[5]Department of Hematology, Oncology and Tumor Immunology, Charité Campus Berlin Buch, 13092 Berlin, Germany
*Correspondence: tblanke@mdc-berlin.de
DOI 10.1016/j.ccr.2011.10.019

SUMMARY

The genetic instability of cancer cells frequently causes drug resistance. We established mouse cancer models, which allowed targeting of an oncogene by drug-mediated inactivation or monospecific CD8$^+$ effector T (T_E) cells. Drug treatment of genetically unstable large tumors was effective but selected resistant clones in the long term. In contrast, T_E cells completely rejected large tumors ($\geq$500 mm^3), if the target antigen was cancer-driving and expressed in sufficient amounts. Although drug-mediated oncogene inactivation selectively killed the cancer cells and left the tumor vasculature intact, which likely facilitated survival and growth of resistant clones, T_E cell treatment led to blood vessel destruction and probably "bystander" elimination of escape variants, which did not require antigen cross-presentation by stromal cells.

INTRODUCTION

One of the hallmarks of cancer is a high degree of genetic instability and the accumulation of somatic mutations. In colorectal cancers, for example, up to 10,000 somatic mutations have been detected (Stoler et al., 1999). The high mutation rate in tumors may explain the frequently observed resistance to chemotherapy or drugs interfering with oncogene activity (Gorre et al., 2001; Knight et al., 2010; Pao et al., 2005). In the clinic, tumors can be detected at about 1 cm in diameter (~500 mm^3), which corresponds to approximately 10^9 tumor cells (Schreiber et al., 2006; Kumar et al., 2004). Anticancer drug efficacy depends on the number of cancer cells and, thus, the number of genetic variants at the time of treatment (Skipper, 1965). Drug and T cell therapy were usually analyzed against small tumors below size that can be detected in the clinic (Schreiber et al., 2006), and their efficacy was never compared in the same tumor model.

If resistance to chemotherapy or oncogene-inactivating drugs is due to selection of mutant clones caused by genetic instability, one would expect that otherwise effective adoptive T cell therapy similarly selects variants that escape T cell-mediated destruction (Liu and Bai, 2008). Antigen loss variants were found in patients with melanoma after T cell therapy (Restifo et al., 1996; Yee et al., 2000), suggesting that T cell therapy is as vulnerable to selection of escape variants as therapy with oncogene-inactivating drugs. However, in some experimental models, adoptively transferred T cells could reject large tumors (defined as $\geq$500 mm^3) (Kast et al., 1989; Spiotto et al., 2004). Sufficient amounts of tumor antigen expression for cross-presentation by tumor stroma cells and T cell-derived interferon-γ (IFN-γ) acting on stroma hindered outgrowth of antigen loss variants (Spiotto et al., 2004; Zhang

Significance

So far, the genetic instability of cancer cells impedes effective therapy with oncogene inactivating drugs as well as adoptively transferred T cells. We created ideal conditions to target the oncogene by drug-mediated inactivation or T cells, which both induced regression of large tumors. Yet, only T cell therapy resulted in long-term cure, probably because the T cells also destroyed the tumor vasculature. Because techniques for therapy with high-avidity T cells against antigens overexpressed in human tumors have recently been developed, defining optimal conditions for T cell therapy may help improve future clinical trials.

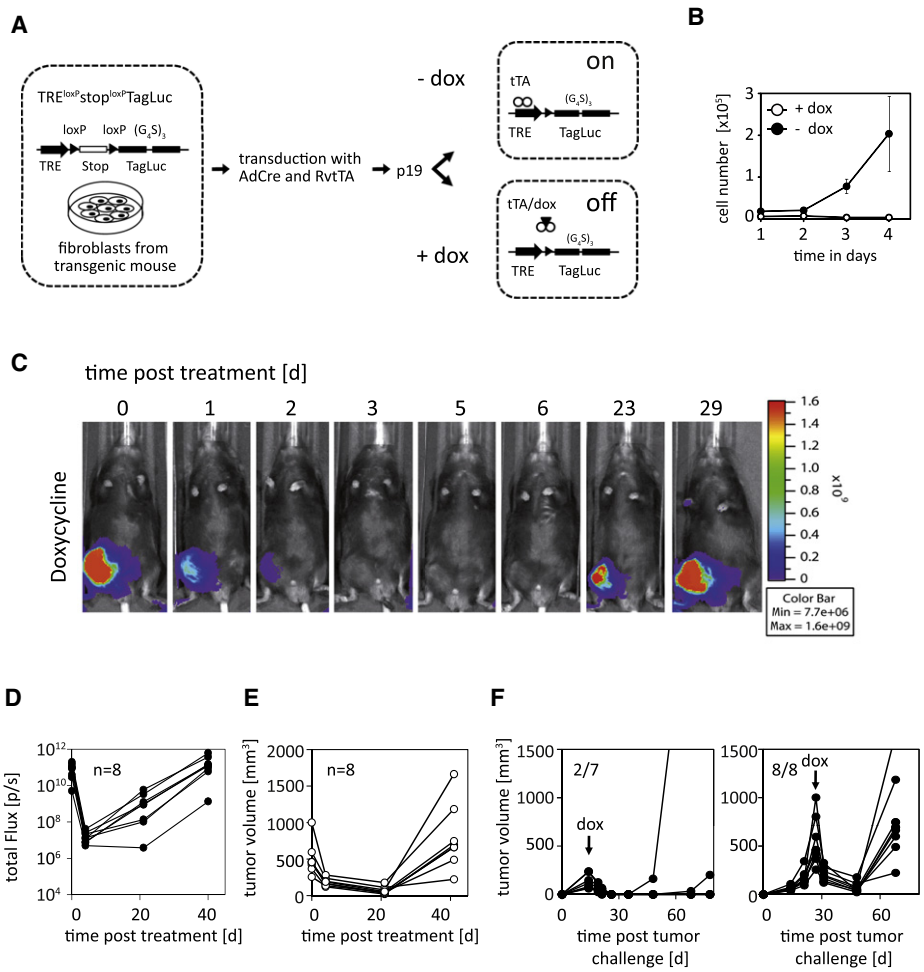

Figure 1. Drug-Mediated Oncogene Inactivation in Large Tumors Induces Transient Tumor Regression

(A) Tet-TagLuc fibrosarcoma cells were generated by infection of primary fibroblasts of a *TRE^{loxP}stop^{loxP}TagLuc* transgenic mouse with a Cre-encoding adenovirus (AdCre) to excise the stop cassette, a Tet-off transactivator-encoding retrovirus (RvtTA), and adaptation to in vivo growth at passage 19 (p19). Expression of the TagLuc fusion gene can be regulated by dox.

(B) Tet-TagLuc cells (1×10^4) in duplicates were cultured with (0.5 μg/ml) or without dox, and cell numbers were determined daily for 4 days. Error bars represent ±SD.

(C) *Rag*$^{-/-}$ mice with established Tet-TagLuc tumors (mean ± SD, 546 ± 246 mm^3 at ~30 days) received dox-containing drinking water, and TagLuc expression was followed by BL imaging (1 s exposure time). The time after treatment is indicated in days (d).

(D) BL signals of dox-treated tumors of individual mice (n = 8) were quantified over time.

(E) Tumor growth kinetics is displayed for mice shown in (D). Results in (C–E) are representative for three experiments with a total of 12 analyzed mice.

(F) Tumor growth kinetics of individual mice (n = 7) with small Tet-TagLuc tumors (≤250 mm^3) treated with dox are shown in the left panel. Time point of dox treatment is indicated. For comparison, the mice with large tumors as in (E) are shown (right panel). The number of mice with tumor relapse is indicated.

et al., 2008). The mode of tumor destruction may be different for drug and T cell therapy that, however, has not been addressed in a clinically relevant (e.g., large) tumor model. Here, we established a mouse cancer model allowing direct comparison of the efficacy of drug versus T cell therapy directed against the same target protein to eradicate large established tumors. SV40 large T antigen (Tag) is a well-characterized oncogene with defined H-2^b restricted epitopes (Staveley-O'Carroll et al., 2003). Tag, among other activities, inactivates the tumor suppressors p53 and retinoblastoma protein (Rb), reducing DNA repair and creating a genetically unstable phenotype (Kuerbitz et al., 1992).

RESULTS

Generation of a Conditional TagLuc Expressing Tumor Cell Line in Mice

To compare the therapeutic efficacy of drug-mediated oncogene inactivation and targeting the oncogene by single peptide antigen-specific CD8$^+$ effector (T_E) cells, we isolated fibroblasts from a *TRE^{loxP}stop^{loxP}TagLuc* transgenic mouse (Figure 1A), which contains the *Tag* gene fused to the firefly luciferase (*Luc*) gene by a linker, encoding glycine-serine $(G_4S)_3$ repeats (*TagLuc*). Expression of the *TagLuc* fusion gene in *TRE^{loxP}stop^{loxP}TagLuc* mice is regulated by a tetracycline response

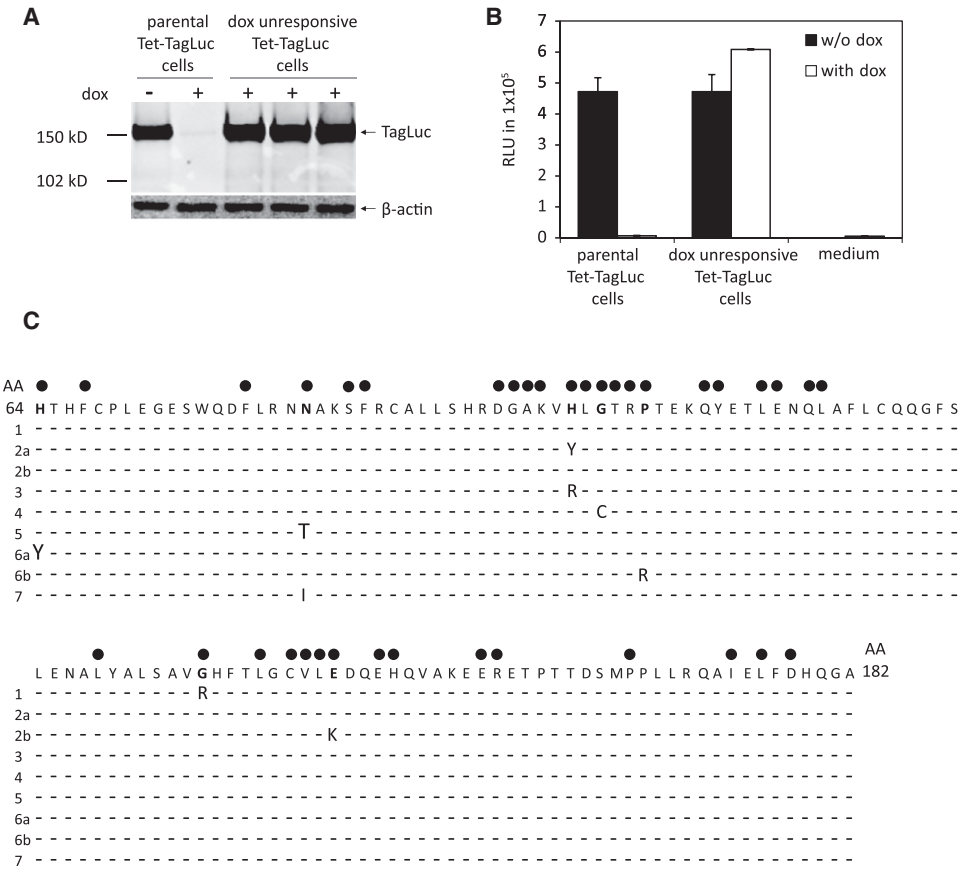

Figure 2. Each Dox-Unresponsive Tumor Reveals a Unique Point Mutation in the Transactivator Gene

(A) Parental Tet-TagLuc cells and cells of three dox-unresponsive tumors were cultured for 5 days in the presence of dox (1 μg/ml), and TagLuc expression was analyzed by western blot analysis with an anti-Tag antibody. As loading control, β-actin was detected.

(B) Relative light units (RLU) were analyzed in parental and drug-resistant Tet-TagLuc cells, cultured in the presence or absence of dox. One of three analyzed dox-unresponsive tumors with similar results is shown. Error bars represent ±SD.

(C) Comparison of the tTA amino acid (AA) sequence from position 64 to182 of parental Tet-TagLuc cells (top) and seven dox-unresponsive tumors (tumor 2 and 6 with two mutations). Mutations are shown in bold. Mutations in the *tTA* leading to dox-unresponsive variants are indicated by a black circle.

element (TRE) and is silent in the absence of an active transactivator (TA) (Gossen and Bujard, 2002). A loxP-flanked stop cassette (between TRE and *TagLuc*) was excised by transient adenoviral Cre recombinase (AdCre) expression in the primary cells (Figure 1A). Subsequent introduction of a Tet-off transactivator (*tTA*) by stable gene transfer with a *tTA*-encoding retrovirus allowed TagLuc expression, reversible by adding doxycycline (dox) (see below). TagLuc-expressing cells at passage 19 of in vitro culture exhibited immortal growth and were adapted to tumor growth in vivo. The resulting cell line, termed Tet-TagLuc, proliferated only in absence of dox (Figure 1B).

TagLuc Inactivation Fails to Control Large Tumors in the Long Term

Mice with large Tet-TagLuc tumors (546 ± 246 mm^3) were treated with dox, and the kinetics of TagLuc inactivation were followed by bioluminescence (BL) imaging. After 1 day, a decrease of BL signal, declining on day 3 below detectable level at 1 s exposure time, was observed, followed by tumor regression. Then, despite further dox treatment, the BL signal reappeared and tumors progressively grew in all cases (Figures 1C–1E). Analysis of the efficacy of dox in treating smaller ($\leq$250 mm^3) tumors showed that most tumors could still be eliminated (Figure 1F), indicating that selection of dox-unresponsive variants that likely occur at a low rate requires large numbers of tumor cells.

Each Dox-Unresponsive Tumor Reveals a Unique Point Mutation in the Transactivator Gene

Tumors that grew in the presence of dox were analyzed in vitro. Although dox treatment of the original Tet-TagLuc cells resulted in loss of TagLuc expression, as shown by western blot and BL analysis, the variant cell lines did not reduce TagLuc expression in response to dox (Figures 2A and 2B), suggesting genetically acquired resistance. These data argued against the possibility that the therapy selected variant cancer cells that lost the oncogene dependence (Jonkers and Berns, 2004; Weinstein, 2002), but rather pointed to the inability of dox to bind to and inactivate the tTA. The amino acid positions in the tTA allowing dox binding are well characterized (Hillen and Berens, 1994; Hinrichs et al., 1994). DNA sequence analysis of seven dox-unresponsive tumors showed in five cases a single point mutation in the *tTA* gene (Figure 2C). Two tumors had two point mutations each,

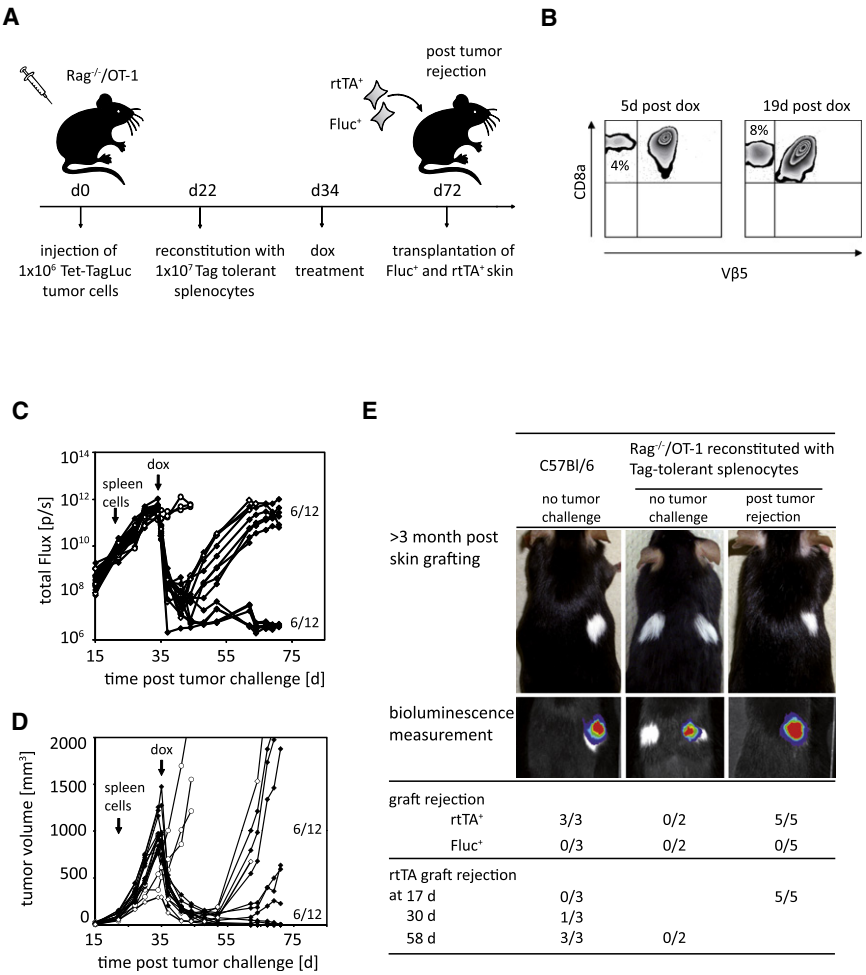

graft rejection			
rtTA+	3/3	0/2	5/5
Fluc+	0/3	0/2	0/5
rtTA graft rejection			
at 17 d	0/3		5/5
30 d	1/3		
58 d	3/3	0/2	

Figure 3. Partial Compensation of Selection of Dox-Unresponsive Tumors by Endogenous T Cells

(A) Scheme of the experimental design. The mice, which rejected the tumor, received two albino B6 skin grafts expressing either the *Luc* or the *rtTA* transgene, both shared with the tumor cells.

(B) Expansion of transferred $CD8^+$ T cells was determined 5 and 19 days after dox treatment by determining the percentage of transferred ($V\beta5^-$) out of total $CD8^+$ T cells (mean ± SD, 4.41 ± 1.64 versus 9.56 ± 1.9; n = 3).

(C) BL signals of tumors (mean ± SD, 892 ± 237 mm^3) were determined over time. (◆) Spleen cell transfer and dox-treatment (n = 12); (○) spleen cell transfer without dox-treatment (n = 3); (◇) dox treatment but no spleen cell transfer (n = 2).

(D) Tumor growth kinetics of mice shown in (C). Numbers of mice with rejected or relapsed tumors are indicated.

(E) Photographs (upper panel) and pictures of BL measurement (middle panel) of Luc^+ (right) and $rtTA^+$ skin grafts (left) transplanted on either C57Bl/6 mice (left), *Rag*$^{-/-}$*/OT-1* mice reconstituted with Tag-tolerant splenocytes that did not (middle) or did receive and reject a tumor after dox treatment (right). Pictures were acquired more than 3 months after skin transplantation. One representative example of each group is shown. Number of graft rejections/number of mice in experiment and time of graft rejection in days (d) is given.

derived from two independent resistant clones. All mutations led to amino acid substitutions in positions known to be binding sites of dox or otherwise essential for tTA function (Hinrichs et al., 1994). Importantly, each tumor had acquired the mutation at a unique tTA-inactivating position or resulting in a different amino acid replacement, showing the high instability of the cancer cells with a seemingly unlimited reservoir of genetic variants in large tumors.

Endogenous T Cells Only Partially Prevent Relapse following TagLuc Inactivation

The previous experiments were performed in *Rag*$^{-/-}$ mice because the C57Bl/6 (B6)-derived Tet-TagLuc cells are rejected in B6 mice as a result of the high immunogenicity of Tag. To ask whether tumor cell death by TagLuc inactivation induced endogenous T cells that counteracted the selection of drug-resistant clones, *Rag*$^{-/-}$*/OT-1* mice bearing 22-day-old (small) tumors received naive splenocytes (Figure 3A). *Rag*$^{-/-}$*/OT-1* mice with tumor-unrelated transgenic (ovalbumin-specific) T cells were used to avoid homeostatic proliferation and nonspecific T cell activation. Splenocytes from Tag-tolerant *LoxP-Tag* × *Alb-Cre* mice were used, because transfer of naive B6 splenocytes led to rejection of these tumors by spontaneously activated Tag-specific T_E cells (our unpublished observation). However, Tet-TagLuc cells express at least two further antigens, Luc and tTA that are foreign to the T cells and could serve as rejection antigens. Tumors in the presence of *LoxP-Tag* × *Alb-Cre* splenocytes progressively grew, showing that Luc and tTA are obviously too weak antigens to spontaneously induce T cells in the reconstituted mice. Following dox treatment on day 34, the tumors (≥500 mm^3) regressed as before, $V\beta5^-$ (non-OT-1) $CD8^+$ T cells expanded (Figure 3B), and half of the mice completely rejected the tumor, whereas in the other half, BL signals increased and the tumor resumed growth (Figures 3C and 3D). In those mice that rejected the tumor, we analyzed whether any of the two putative tumor antigens had induced T cells because of TagLuc inactivation-induced tumor cell death, which contributed to tumor rejection. Therefore, mice received two skin grafts, either from *CAG-FLuc* or *rtTA-CM2* transgenic mice. In both cases, the transgene is expressed by the ubiquitous CAG promoter. For better transplant visibility, albino B6 mice were used as transgenic skin donors. T cell-reconstituted *Rag*$^{-/-}$*/OT-1* mice that had not received Tet-TagLuc cells long term accepted both skin grafts (Figure 3E). Naive B6 mice rejected the rtTA but long term accepted the Luc skin graft. Reconstituted *Rag*$^{-/-}$*/OT-1* mice that had rejected Tet-TagLuc tumors after dox-induced TagLuc inactivation rejected the rtTA but not the Luc skin graft. In these mice, the *rtTA* skin graft was rejected faster than in naive B6 mice, suggesting that rtTA-specific memory T cells had been induced during tumor cell death (Figure 3E). These data suggested that endogeneous

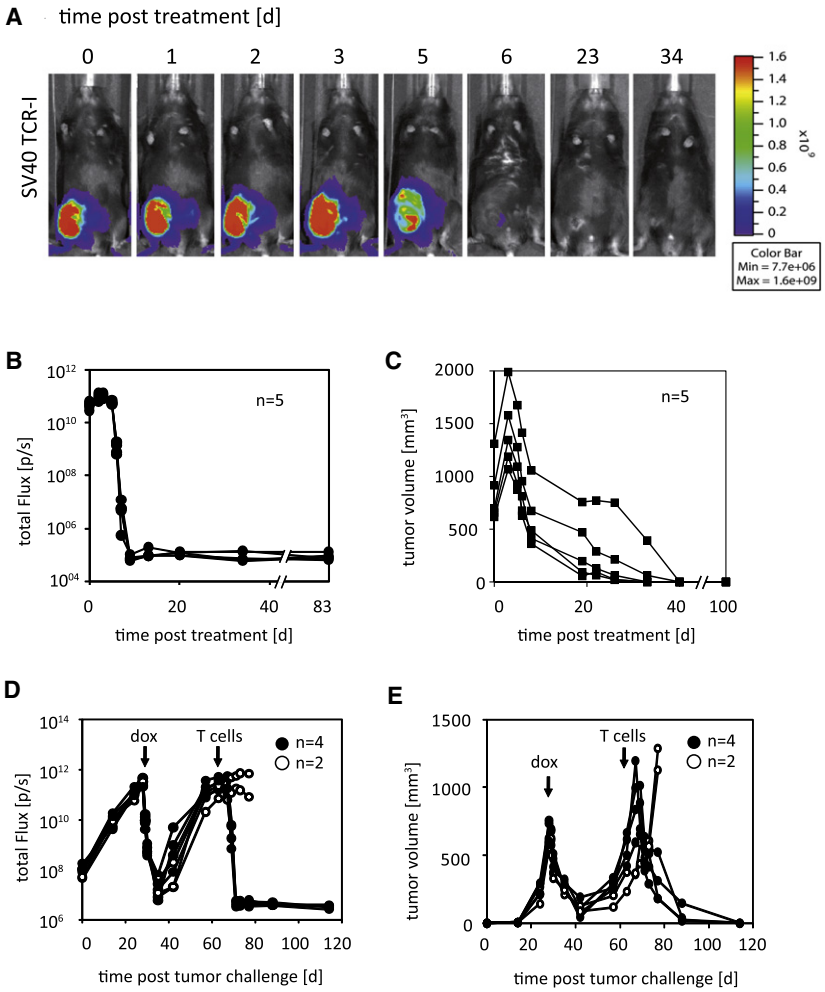

Figure 4. Complete Eradication of large Genetically Unstable Tumors by Adoptive T Cell Therapy with Single Peptide-Specific T_E cells

(A) *Rag*$^{-/-}$ mice with established Tet-TagLuc tumors (mean ± SD, 837 ± 287 mm^3) received 1 × 10^6 TCR-I T_E cells, and changes of TagLuc signal were followed by BL imaging (1 s exposure time). The time after treatment is indicated in days (d). See also Figure S1.

(B) BL signals of T_E cell-treated tumors of individual mice (n = 5) were measured over time.

(C) Tumor growth kinetics of mice shown in (B). Results in (A–C) are representative for three experiments with a total of 10 analyzed mice.

(D) *Rag*$^{-/-}$ mice with established Tet-TagLuc tumors (mean ± SD, 643 ± 82 mm^3) were treated with dox, and relapsed tumors (6/6) were subsequently treated by T_E cells (●; n = 4) or were left untreated (○; n = 2). Changes in BL signal over time of individual mice are shown.

(E) Tumor growth kinetics of mice shown in (D). One representative of two experiments with a total of eight double-treated mice is shown.

T cells only partially prevented tumor relapse following TagLuc inactivation, even though the tumor expressed a skin graft rejection antigen.

Complete Eradication of Large Tumors by Single Peptide-Specific CD8$^+$ Effector T Cells

Next, we asked whether adoptive T cell therapy with T_E cells directed against the epitope I of Tag (Staveley-O'Carroll et al., 2003) also selected escape variants, when used to treat large tumors. The epitope I region is dispensable for the transforming activity of Tag, and epitope I loss variants of murine fibrosarcoma cells could be selected in vitro by specific T cells (Mylin et al., 2007). Also, H-2 loss variants of Tag-transformed cells were found in transiently immune-suppressed mice (Gooding, 1982). Thus, escape variants of Tet-TagLuc cells under T_E cell pressure appeared likely, in light of the high genetic instability and large number of tumor cells at the time of treatment. Epitope I-specific (purified TCR-I transgenic) T_E cells (Figure S1 available online) were transferred into mice with large established Tet-TagLuc tumors (≥500 mm^3), and tumor regression was followed by BL imaging. In contrast to dox treatment, no decrease in BL signal was observed within the first 4 days after T_E cell injection, and tumors even increased in size (Figures 4A–4C). Then, between days 5 and 6, the BL signal dramatically decreased and became undetectable, accompanied by hemorrhagic necrosis of the tumor that was not seen in the dox-treated tumors. T_E cell-treated mice in all cases completely rejected the tumor (Figure 4C). In another experiment, mice with Tet-TagLuc tumors were treated with dox as before and, when large drug-resistant tumors had developed, were treated with T_E cells, causing complete and long-term tumor rejection in all mice (Figures 4D and 4E). Thus, T_E cells with single peptide specificity reject large tumors, even those that had developed drug resistance, despite large genetic instability.

T_E Cells but Not TagLuc Inactivation Eradicates Gastric Carcinomas in Mice

One cannot exclude that the effective T_E cell treatment of Tet-TagLuc tumors was because this cell line was generated by in vitro transformation and had not undergone in vivo evolutionary processes. Previously, we had observed in another transgenic mouse model with a dormant Tag oncogene that, by stochastic rare events, sporadic tumors developed as a result of somatic mutations or epigenetic events (Willimsky and Blankenstein, 2005; Willimsky et al., 2008). Therefore, *TRE*^{loxP} *stop*^{loxP}*TagLuc* mice were crossed to *rtTA* (tet-on) transactivator transgenic (*rtTA-CM2*) mice. A small cohort of double transgenic mice (with the stop cassette present) was kept on dox, and BL signals were determined over time (Figure 5A). A distinct BL signal appeared in one mouse after 411 days of dox treatment that derived from a sporadic gastric carcinoma that was Luc and Tag positive (Figures 5B and 5C). Proliferation of a cell line (TC200.09) derived from this tumor depended on the presence of dox (Figure 5D). Large established TC200.09 tumors were treated with dox withdrawal or T_E cells. TagLuc inactivation led

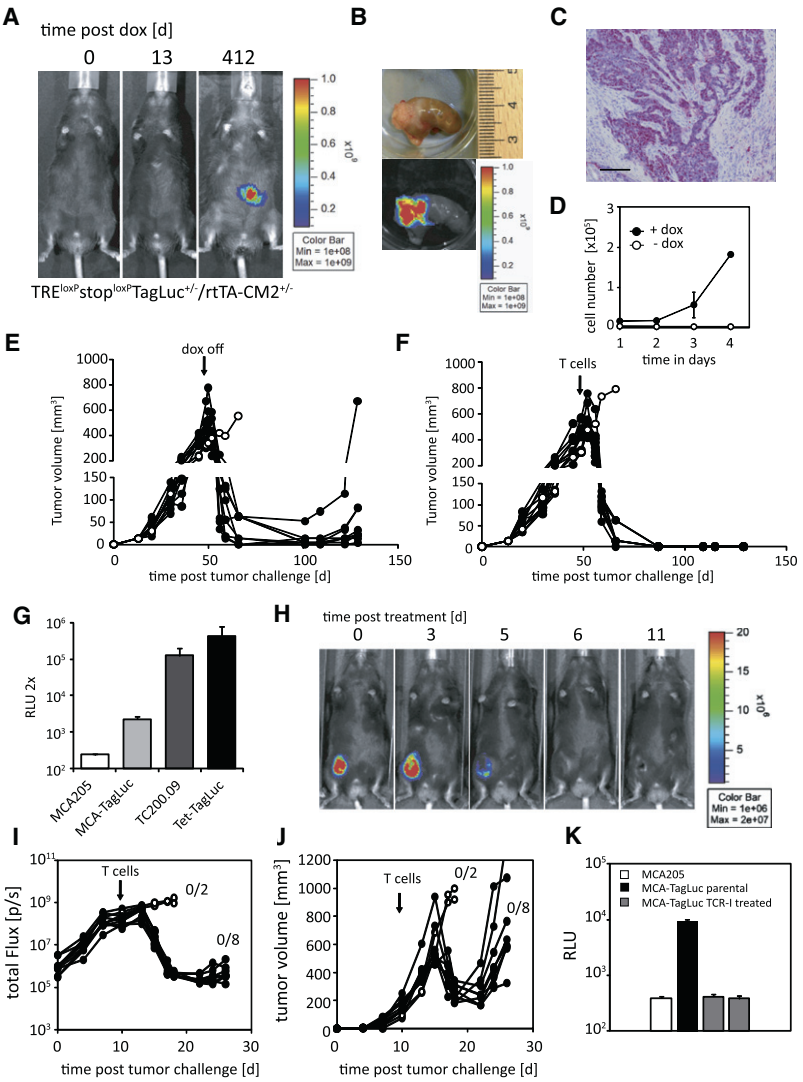

Figure 5. Drug but Not T_E Cell Resistance of Gastric Carcinoma and Dependence of T Cell Therapy on TagLuc Expression Level

(A) Sporadic tumor development was monitored in a *TRE^{loxP}stop^{loxP}TagLuc$^{+/-}$/rtTA-CM2$^{+/-}$* double transgenic mouse by BL imaging. Time after starting dox administration in days (d) is indicated.

(B) A tumor, located on the outer wall of the stomach fundus, was isolated from the mouse shown in (A). A photograph (upper panel) and a BL image (lower panel) were acquired ex vivo.

(C) A section of the isolated stomach tumor was stained with anti-Tag antibodies (scale bar, 100 μm).

(D) Proliferation of 1 × 10^4 cells (TC200.09) from the stomach tumor was analyzed in the presence and absence of dox in duplicates for 4 days. Standard deviation (SD) is indicated.

(E) *Rag*$^{-/-}$ mice with established TC200.09 tumors (mean ± SD, 453 ± 110 mm^3 at day 49) were left untreated (○; n = 1) or treated by dox withdrawal (●; n = 9) and tumor growth kinetics was determined.

(F) *Rag*$^{-/-}$ mice with established TC200.09 tumors (mean ± SD, 435 ± 100 mm^3 at day 49) were left untreated (○; n = 1) or were treated with T_E cells (●; n = 10) and tumor growth kinetics was determined. Arrows in (E and F) indicate time point of treatment.

(G) TagLuc expression in MCA-TagLuc, TC200.09, and Tet-TagLuc tumor cells was determined by quantifying relative light units (RLU) in 5 × 10^5 cells (duplicates). Data represent mean values from three independent experiments (±SD).

(H) *Rag*$^{-/-}$ mice with small MCA-TagLuc tumors (mean ± SD, 166 ± 55 mm^3 ten days after cell injection) received T_E cells as before and loss of TagLuc signal was followed by BL imaging.

(I) BL signals of T_E cell-treated (●; n = 8) or untreated MCA-TagLuc tumors (○; n = 2) in individual mice were measured over time.

(J) Tumor growth kinetics of mice shown in (I) shows outgrowth of escape variants. Number of mice with tumor rejection per total number of mice is indicated. One representative of two experiments is shown. Error bars in (D), (G), and (K) represent ±SD.

(K) RLU were analyzed in MCA205, parental MCA-TagLuc cells and two tumors that escaped T_E cell treatment.

to tumor regression, but in some mice (3/9) tumors resumed growth after more than 2 months, and in the other mice tumors did not completely regress 80 days after treatment (Figure 5E). Dox treatment of some of these mice (2/9) rapidly induced BL signals (data not shown), suggesting incomplete tumor cell elimination after TagLuc inactivation. In contrast, T_E cells completely rejected the tumor in all mice (Figure 5F).

Selection of Antigen Loss Variants by T_E cells, if TagLuc Is Not Cancer-Driving and Expressed in Lower Amounts

To ask whether epitope I-specific T_E cells can select TagLuc-negative variants in general, MCA-205 fibrosarcoma cells, transfected to express ~25- and 100-fold lower amounts of the TagLuc antigen (MCA-TagLuc) in comparison to TC200.09 and Tet-TagLuc cells, respectively, were established (Figure 5G). When mice with comparably small MCA-TagLuc tumors (166 ± 55 mm^3) were treated with T_E cells, BL signals disappeared after 5–6 days as before and tumors regressed (Figures 5H–5J). Then, however, tumors resumed growth without proportional increase in BL signal. These tumors had lost TagLuc expression, as verified by in vitro analysis (Figure 5K). Thus, if the target antigen is expressed at lower level and/or is not cancer-driving, escape variants are easily selected.

Different Mode of Tumor Cell Death by TagLuc Inactivation and T_E Cells

We searched for differences in tumor destruction induced by TagLuc inactivation and T_E cell treatment that can explain why escape variants occurred upon drug but not T_E cell treatment of Tet-TagLuc tumors. Before treatment, tumors had a high-grade pleomorphic sarcoma phenotype with few apoptotic cells and many mitoses (Figure S2). Four days after dox treatment, tumors had a fascicular growth pattern with spindle cell morphology resembling low-grade fibrosarcoma. The cell density decreased, and Tag and Luc expression were undetectable apart from few focal areas, consistent with loss of expression of the proliferation marker Ki-67 (Figure 6A). On day 7 after dox treatment, almost no Tag- or Luc-positive cells were detected,

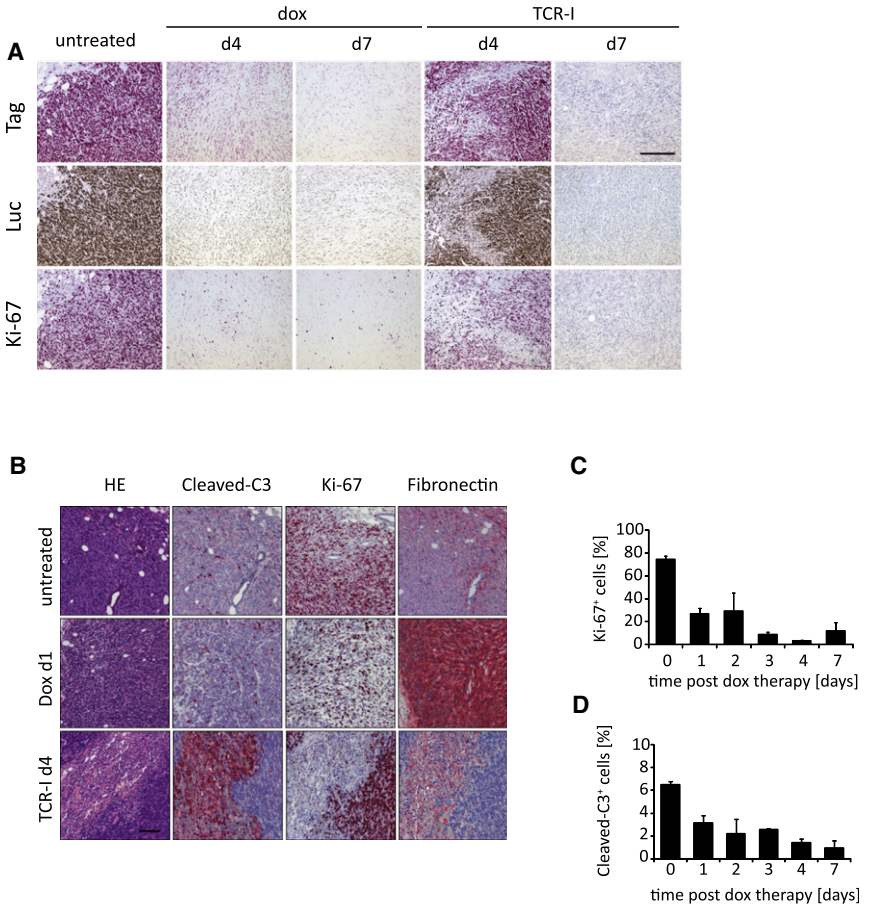

Figure 6. T_E Cells Kill by Apoptosis Induction, Whereas TagLuc Inactivation Induces Autophagy

(A) Consecutive Tet-TagLuc tumor sections were stained with antibodies against Tag, luciferase, and Ki-67 at the indicated days (d) after therapy. See also Figure S2.

(B) Consecutive sections of untreated (n = 3), dox-treated (day 1 after therapy; n = 3), or T_E cell-treated tumors (day 4 after therapy; n = 3) were stained with HE and antibodies against cleaved Caspase 3 (cleaved-C3), Ki-67, and fibronectin. Scale bar in (A) and (B), 100 μm.

(C) Quantification of Ki-67$^+$ cells at different time points after TagLuc inactivation.

(D) Quantification of cleaved-C3$^+$ cells at different time points after TagLuc inactivation. A total of 1,000 cells in five nonoverlapping high-power fields were counted in (C) and (D) for each time point. Three tumors per time point were analyzed. For day 7, two tumors were analyzed.

(E) Tet-TagLuc cells were treated in vitro with dox or were left untreated. After the indicated time points, cells were stained with Annexin V and propidium iodide (PI). Mean values from two experiments are shown (±SD).

(F) Tet-TagLuc cells were cultured in the absence or presence of dox as indicated, and indicated proteins were analyzed by immunoblotting. Equal protein loading was confirmed by β-actin detection. See also Figure S2. Error bars in (C–E) represent ±SD.

and the cell density was very low embedded in a myxoid matrix. To elucidate the mechanism of tumor cell decrease upon TagLuc inactivation, Ki-67$^+$ cells were enumerated over time, revealing a loss of cell proliferation as early as 1 day following dox application (Figures 6B and 6C). Surprisingly, cleaved Caspase3 (C3)$^+$ cells did not increase but, if at all, decreased after TagLuc inactivation, arguing against apoptotic cell death (Figures 6B and 6D). This was supported by in vitro experiments showing an increase of Annexin V$^+$/propidium iodide$^+$ cells after TagLuc inactivation, but not single Annexin V$^+$ cells, as an intermediate step during apoptotic cell death (Figure 6E). After 7 days of dox treatment, cell numbers decreased by 83% (our unpublished observation). However, 1 day after dox application, Tet-TagLuc tumors strongly upregulated fibronectin expression in vivo (Figure 6B). Expression of fibronectin has been associated with cell differentiation and cellular senescence, but it has also been shown that fibronectin expression is upregulated by light chain 3 (LC3) microtubule-associated proteins (Ying et al., 2009). A shift of LC3 from a soluble to a membrane-bound form (LC3-II) is a marker of autophagy (Kabeya et al., 2000). TagLuc inactivation in vitro led to a rapid increase in LC3-II but not cleaved-C3 expression (Figure 6F). Expression of p62 but not Beclin-1 gradually decreased over time (Figure S2). Thus, TagLuc inactivation results primarily in autophagic but not apoptotic cell death.

In contrast, tumors from mice treated with T_E cells 4 days earlier contained largely viable tumor cells that stained positive with antibodies against Tag, Luc, and Ki-67, consistent with the BL imaging (Figure 6A). Few focal necrotic areas (less than 10%) were observed. These areas appeared to mark the beginning of tumor eradication, as has been suggested (Blohm et al., 2006). Areas of apparent tumor cell death stained positive for cleaved-C3 but not Ki-67 or fibronectin (Figure 6B). Adjacent tumor tissue revealed the opposite staining pattern, indicating that the T_E cells moved through the tumor in distinct clusters leaving apoptotic tumor cells behind. On day 7, tumors were completely necrotic (Figure 6A).

T_E Cell Treatment but Not TagLuc Inactivation Destroys the Tumor Vasculature

Macroscopically, regressing Tet-TagLuc tumors appeared differently after dox and T_E cell treatment, respectively. In contrast

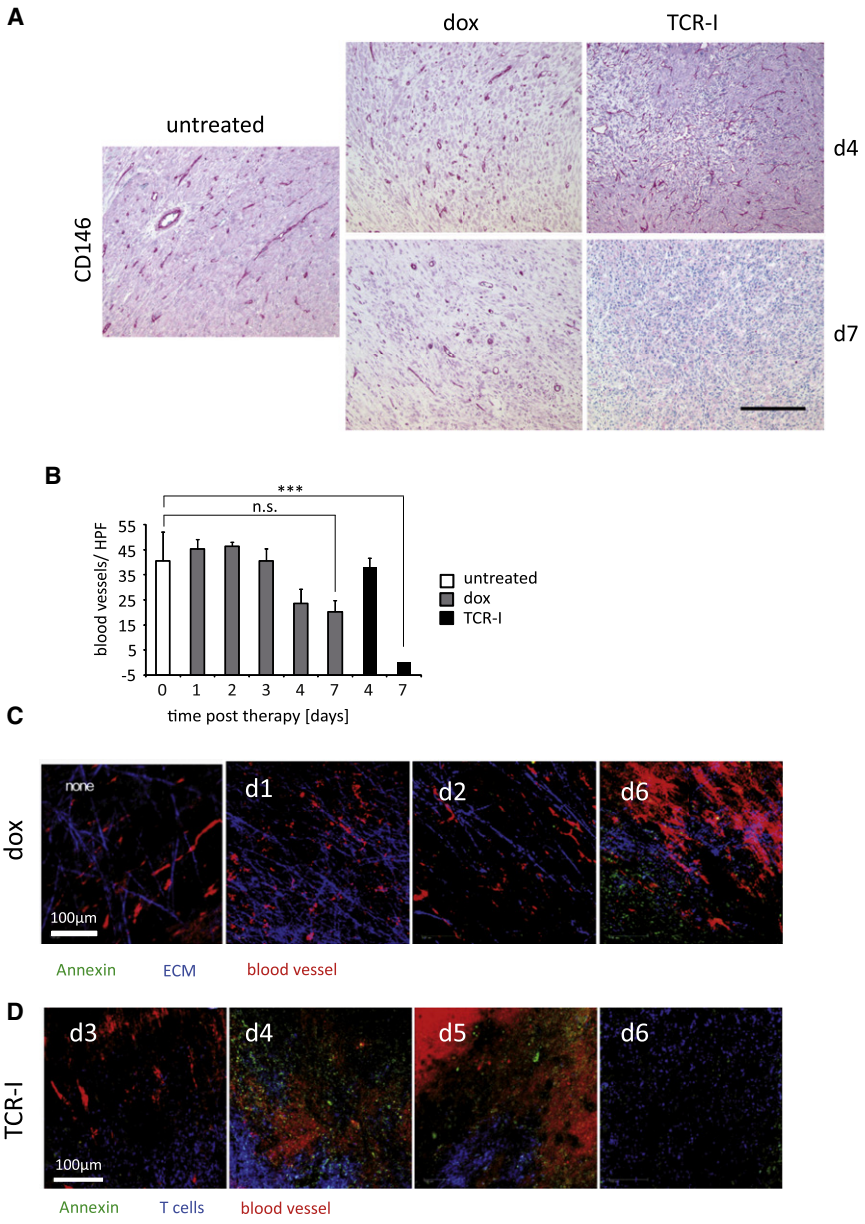

Figure 7. T_E Cell Treatment but Not TagLuc Inactivation Leads to Destruction of the Tumor Vasculature

(A) Tet-TagLuc tumor sections were stained for the endothelial cell marker CD146 at the indicated days (d) after start of therapy (scale bar, 100 µm). See also Figure S3.

(B) Quantification of blood vessels ($CD146^+$) in sections of untreated (n = 3), dox-treated (d1 to d3 and d7, n = 2; d4, n = 3) and T_E cell-treated (d4 and d7, n = 3) tumors (mean of 5 HPF at 400-fold magnification). Error bars represent ±SD. ***p 0.001; n.s. not significant (p 0.372); t test with Bonferroni correction.

(C) IVMPM of blood vessels (red), extracellular matrix (ECM; blue), and Annexin V^+ cells (green) subsequent to dox administration for time points as indicated.

(D) IVMPM of blood vessels (red), adoptively transferred $CD8^+$ cells (blue), and Annexin V^+ cells (green) subsequent to adoptive T cell transfer for time points as indicated. Scale bar, 100 µm.

to dox-treated tumors, T_E cell-treated tumors became necrotic when BL signals had disappeared, pointing to differential effects on the tumor vasculature (Figure S3). Immunohistochemical analysis revealed that tumor blood vessels ($CD146^+$) only slightly (2-fold) decreased in Tet-TagLuc tumors 4 and 7 days after oncogene inactivation (Figures 7A and 7B). At 4 days after T_E cell treatment, tumor vasculature was not significantly reduced. Then, 7 days after T_E cell transfer, the whole tumor tissue was necrotic and endothelial cells were not detected anymore (Figures 7A and 7B). Thus, a major difference between the two therapies appears to be the destruction of the tumor vasculature, in addition to tumor cells, by T_E cells but not by drug therapy. To directly visualize T_E cells destroying tumor blood vessels, intravital multiphoton microscopy (IVMPM) was used. Before treatment, tight blood vessels were seen and no egression of dextran-rhodamine was observed (Figure 7C). On day 3 after T_E cell transfer, T cells entered distinct areas of the tumor in clusters but blood vessels remained still intact (Figure 7D). After 4 and 5 days, blood vessels were destroyed in areas of T cell infiltration, as shown by egress of dextran-rhodamine, and apoptotic (Annexin V^+) cells became visible. Six days after T_E cell transfer, only T cells were left and no dextran-rhodamine or Annexin V^+ cells were detectable, suggesting that blood vessels and tumor cells are almost simultaneously destroyed at sites of T_E cell infiltration. One and 2 days after dox treatment, normal blood vessels and extracellular matrix (ECM) fibers, indicative of healthy tumor tissue, were observed (Figure 7C). On day 6, tumors contained abundant Annexin V^+ cells and absence of tensed ECM fibers, indicating stromal instability as a result of tumor cell death. Blood vessels were largely retained, even though some egress of dextran-rhodamine was observed, likely as a consequence of vascular remodeling subsequent to tumor cell death.

T_E Cells Destroy the Tumor Vasculature and Long-Term Reject Tumors Without Antigen Cross-Presentation by Stroma Cells

Bystander elimination of escape variants by T_E cells has been shown to require antigen cross-presentation by tumor stroma cells (Spiotto et al., 2004). In these models, as opposed to ours, a non-cancer-driving antigen was used, which may allow an easier selection of escape variants. Therefore, we asked whether blood vessel destruction and tumor rejection by T_E cells required antigen cross-presentation. T_E cells, sorted to high

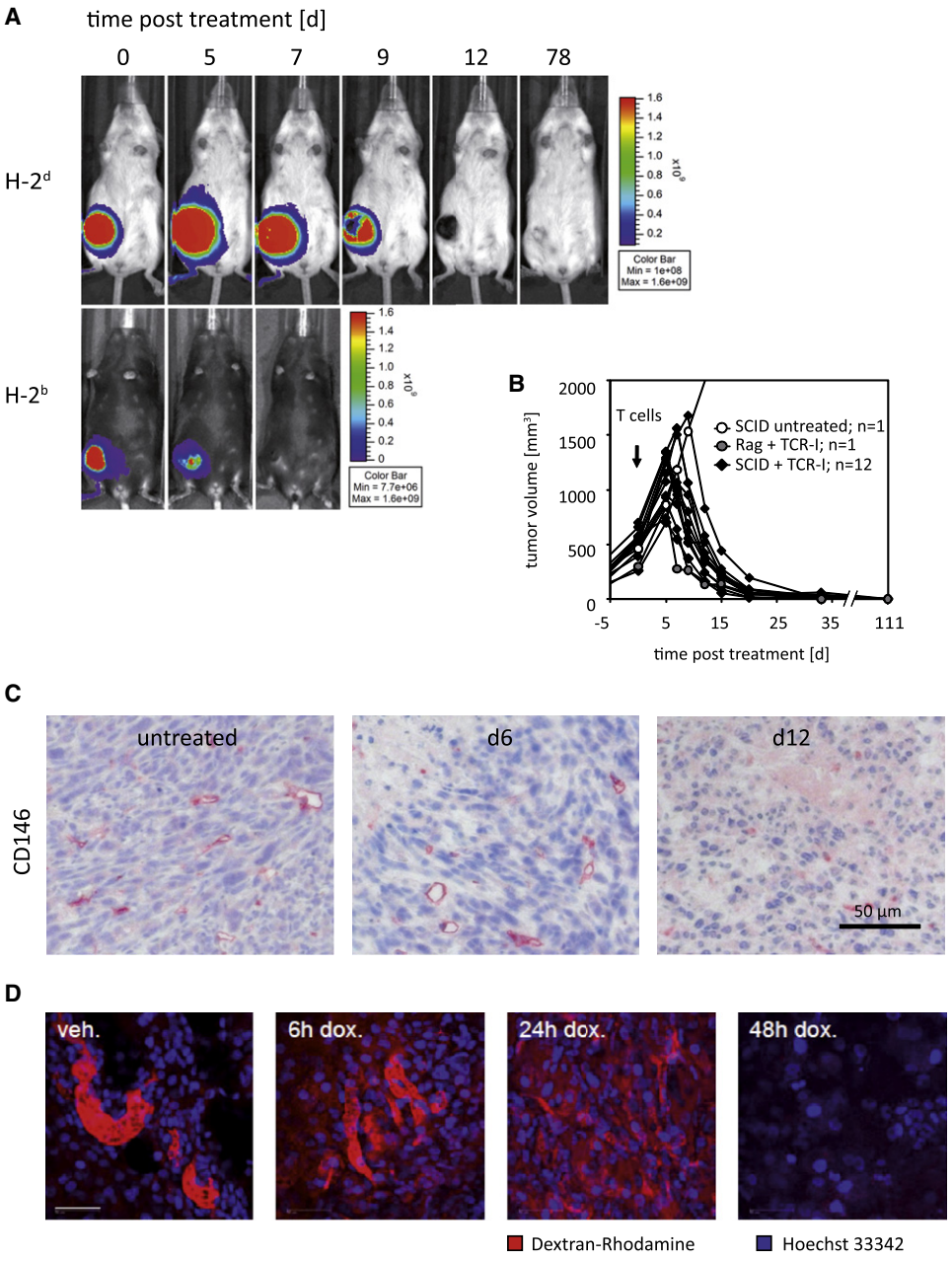

Figure 8. Antigen Cross-Presentation Is Dispensable for Rejection of Large Tet-TagLuc Tumors by T_E Cells

(A) *SCID* mice (H-2^d) with established Tet-TagLuc tumors (mean ± SD, 521 ± 118 mm^3 26 days after cell injection) were treated with H-2 D^b restricted T_E cells, and changes of TagLuc signal were monitored by BL imaging (1 s exposure time). One representative example of 12 analyzed mice is shown. For comparison, BL signal change in a tumor, growing in an identically treated *Rag*$^{-/-}$ mouse (H-2^b), is shown. See also Figure S4.

(B) Kinetics of tumor rejection in T_E cell-treated (n = 12) or untreated *SCID* (n = 1) and T_E cell-treated *Rag*$^{-/-}$ mice (n = 1).

(C) Tumors were isolated from untreated *SCID* mice (n = 3) or 6 (n = 2) and 12 days (n = 1) after T_E cell therapy and stained for the endothelial cell marker CD146.

(D) *Rag*$^{-/-}$ mice with established J558L-IFN-γ^{IND} tumors (mean ± SD, 200 ± 40 mm^3 at day 7; n = 4) received 10 µg of dox i.p. for local IFN-γ production. Integrity of the tumor vasculature was analyzed at indicated time points after dox treatment by IVMPM.

purity according to transgenic Vβ7 expression (Figure S4), were transferred into H-2^d severe combined immune deficiency (*SCID*) mice bearing large established H-2^b Tet-TagLuc tumors, so that the T_E cells could recognize the antigen exclusively on the tumor cells. Unlike in H-2^b tumor-bearing *Rag*$^{-/-}$ mice, in which BL signals started to decrease at day 5 after T_E cell transfer and had disappeared on day 7, BL signals did not decrease in *SCID* mice until day 7. An example is shown in Figure 8A and all data in Figure S4. Starting on day 9 after T_E cell transfer, BL signals of Tet-TagLuc tumors decreased in *SCID* mice and then became undetectable, concomitant with long-term tumor rejection (Figure 8B) and expansion of the transferred (D^b/peptide I tetramer

molecule$^+$) T_E cells (Figure S4). Similar results were obtained with immune spleen cells isolated from *TCR-I/Rag*$^{-/-}$ mice (our unpublished observation). Compatible with the BL analysis, CD146$^+$ endothelial cells were present on day 6 after T_E cell transfer in Tet-TagLuc tumors but had been destroyed on day 12 (Figure 8C). Thus, blood vessel destruction and tumor rejection does not require antigen cross-presentation by tumor stroma cells in the Tet-TagLuc model.

Local IFN-γ Production Within Established Tumors Is Sufficient for Rapid Blood Vessel Destruction

Finally, we asked how T_E cells are able to destroy the tumor vasculature without recognizing the tumor antigen on the tumor stroma (e.g., endothelial cells). A major effector molecule by T_E cells is IFN-γ, which is also produced by epitope I-specific T_E cells upon antigen recognition (our unpublished observation). IFN-γ can prevent recruitment of endothelial cells during establishment of solid tumors (Qin and Blankenstein, 2000; Qin et al., 2003), but its effect on established tumor vasculature is less clear. Therefore, we used a tumor cell line (J558L-IFN-γ^{IND}) that allowed the induction of IFN-γ in established tumors by dox (Briesemeister et al., 2011). Thereby, we mimicked the effect of a single T_E cell-derived effector molecule on the tumor vasculature, visualized by IVMPM in tumor-bearing mice injected with dextran-rhodamine. Before dox treatment, tight blood vessels in J558L-IFN-γ^{IND} tumors were observed and no dextran-rhodamine leaked out of the vessels (Figure 8D). As early as 6 hr and more markedly after 24 hr of local IFN-γ induction by dox injection, dextran-rhodamine leaked from the blood vessel. After 48 hr, no dextran-rhodamine was observed in the tumors, indicating that local induction of IFN-γ in established tumors was sufficient to rapidly destroy the tumor vasculature (Figure 8D).

DISCUSSION

We compared the efficacy of drug-induced oncogene inactivation versus T cell therapy against large tumors and defined conditions that support or impede either form of therapy. Drug therapy was modeled by dox-inducible inactivation of a fusion protein between Tag and Luc, allowing sensitive in vivo imaging of oncogene expression. Several transgenic models allowing dox-controllable oncogene inactivation, such as myc, ras, Her-2, and bcr-abl, have been described (Chin et al., 1999; Felsher and Bishop, 1999; Huettner et al., 2000; Moody et al., 2002). Similar to the Tet-TagLuc model, oncogene inactivation always resulted in tumor regression, demonstrating that the concept of oncogene addiction, the long-term dependency of the tumor on a single oncogene, applies to a variety of different oncogenes and tumor types (Jonkers and Berns, 2004; Weinstein, 2002). Primary tumors behaved similarly to transplanted tumors (Felsher and Bishop, 1999). Drug-resistant tumors have been observed in most models, albeit with variable frequency, which could be due to tumor load (e.g., most small but not large Tet-TagLuc tumors were successfully treated). Alternatively, it may be inherent to the cancer-driving oncogene, differences in the mode of tumor cell death upon oncogene inactivation, or differences in *tTA* copy numbers. Drug-resistant tumors transformed by ras, myc, or Her-2 in most cases did not express the oncogene, indicating that dox regulation still functioned and that these tumors had activated alternative transforming pathways (Chin et al., 1999; Felsher and Bishop, 1999; Moody et al., 2002). In contrast, we found inactivating point mutations in the *tTA* gene and persistent TagLuc expression in all drug-resistant Tet-TagLuc tumors. This could either mean that TagLuc-transformed tumors are less prone to the activation of alternate transforming pathways or exhibit more genetic instability (e.g., because of the p53 and Rb inactivating activity mediated by Tag). In the clinic, both drug-inactivating mutations (e.g., in tyrosine kinase genes) and other mechanisms that do not involve mutations in the target oncogene have been found under drug therapy (Knight et al., 2010).

Current models of oncogene inactivation implicated apoptosis in tumor regression. We failed to obtain evidence of apoptosis in Tet-TagLuc cells following TagLuc inactivation. Instead, tumor cell death was associated with autophagy. Autophagy has been suggested as a survival and a death factor during drug therapy (Kondo et al., 2005). The concomitant induction of autophagy and tumor cell death within a few days after TagLuc withdrawal suggests that autophagy contributed to tumor cell death, but we cannot exclude that it also supported the selection of drug-resistant clones. In previous models, apoptosis has been analyzed by the TUNEL assay, which measures DNA fragmentation. However, the TUNEL assay does not distinguish between apoptotic and nonapoptotic cell death. Therefore, it remains to be seen whether oncogene inactivation-induced autophagic cell death is a unique feature of TagLuc inactivation or whether it also occurs for other oncogenes and whether the tumor cell type influences the mode of antistress response caused by oncogene withdrawal.

Two forms of non-cell autonomous effects during drug-induced tumor cell death have been described. Cytotoxic drugs were more efficient in T cell-competent compared to T cell-deficient mice (Casares et al., 2005; Uckert et al., 1998). Although we found indications of "immunogenic cell death" following TagLuc inactivation in large tumors, only some of the mice rejected the tumor in the presence of endogenous T cells, even though the tumor expressed tTA as (skin graft) rejection antigen. Recently, it was shown that CD4$^+$ T cells sustained tumor regression upon myc inactivation (Rakhra et al., 2010). It is unclear why tumor rejection after myc inactivation in the presence of T cells was more efficient, because this model differed from ours in several factors, such as tumor type (lymphoma versus sarcoma), genetic background (FVB versus B6 mice), experimental setup, and, possibly, tumor immunogenicity. In both tumor models, Luc and tTA were expressed as foreign antigens, but it is unknown how immunogenic the two antigens are in FVB mice. We think that the time the tumor had grown before oncogene inactivation is a critical factor, whether or not tumor cell death is immunogenic, because the frequently observed tumor-induced T cell tolerance requires a certain time of antigen exposure. In this regard, both the myc-driven and the Tag-driven model do not reflect the clinical situation, in which T cells are exposed to the tumor for a longer time. Although human tumors carry many mutations and, thus, potentially foreign antigens, it is not known how many are in fact immunogenic and how strong they are. Proof of "immunogenic cell death" upon oncogene inactivation in the clinic is still lacking. A second non-cell autonomous effect, reported in a model of ras inactivation, is the

reduction of tumor endothelial cells within oncogene-deprived tumors (Chin et al., 1999; Tang et al., 2005). We also noted a slight (2-fold) reduction in the number of endothelial cells, but large numbers were still present when most tumor cells had disappeared at 7 days after TagLuc inactivation.

Each drug-resistant Tet-TagLuc tumor carried a unique inactivating mutation in the *tTA* gene, caused by the high genetic instability of the cancer cells and the stochastic accumulation of mutations with increasing tumor burden. Therefore, variants with mutations in epitope I, loss of MHC class I, or those employing other escape mechanisms (Gooding, 1982; Mylin et al., 2007) likely also occurred in large Tet-TagLuc tumors. However, the major difference in tumor elimination by TagLuc inactivation and T_E cell therapy appeared to be the complete destruction of the tumor vasculature and probably the whole tumor stroma by T_E cells, whereas TagLuc inactivation selectively killed the cancer cells but left most endothelial cells alive. We propose that variants that escaped drug therapy have a high chance to survive, because they are embedded in a vital stroma. In contrast, within the T_E cell-induced necrotic tumor tissue immune escape variants are unlikely to survive.

"Bystander killing" of antigen loss variants required enough amounts of antigen for cross-presentation by tumor stroma cells and IFN-γ, which is produced by T cells upon antigen recognition, acting on stroma cells (Spiotto et al., 2004; Zhang et al., 2008). Compatible with these data, antigen loss variants of comparably small MCA-TagLuc tumors that expressed TagLuc in lower amounts and in a non-cancer-driving fashion compared to Tet-TagLuc and TC200.09 cells escaped T_E cells. Surprisingly, complete rejection of large Tet-TagLuc tumors did not require antigen cross-presentation by tumor stroma cells. Infiltration of Tet-TagLuc tumors by large numbers of T_E cells started in distinct tumor areas, where apoptosis of tumor cells and blood vessel destruction occurred simultaneously. Previously, it was shown in a model with low numbers of tumor cells (3-day-old B16-Ova cells) that antigen recognition by T_E (*OT-1*) cells on the tumor cells was sufficient to eliminate the tumor cells, which required IFN-γ responsiveness of host cells (Schüler and Blankenstein, 2003). This was explained by a three-cell interaction, in which T_E cells upon antigen recognition on the tumor cells produced IFN-γ, which inhibited endothelial cells and prevented tumor establishment (Blankenstein, 2005). Because IFN-γ expression in established tumors was sufficient to rapidly destroy the tumor vasculature, we suggest that, in the Tet-TagLuc tumor model, antigen recognition by T_E cells on the tumor cells induces cytokines such as IFN-γ or TNF-α (Zhang et al., 2008), which destroy the tumor vasculature, thereby inducing necrosis and elimination of escape variants. It is unclear why such a three-cell interaction and cytokine-mediated blood vessel destruction was not operative in MCA-TagLuc tumors or other tumor models (Spiotto et al., 2004). The type of antigen (epitope), the quality of the T_E cells, antigen amount-dependent effector functions of the T_E cells in the tumor microenvironment, the cancer-driving nature of the target antigen, or a combination of these factors may account for the differences.

With regard to drug therapy and resistance, our model bears large similarities to the clinical situation. Human cancer is frequently characterized by genetic instability. Resistance to drugs, which target oncogenic pathways, is a common observation in the clinic. The treatment of large clinical-size tumors and the drug resistance caused by the high genetic instability in our model closely resembles the clinical experience. With regard to T_E cell therapy, our model only partially resembles the clinical experience. Although individual cases of long-term regression have been observed, immune escape in patients with melanoma upon T_E cell therapy frequently occurs (Restifo et al., 1996; Yee et al., 2000). By targeting a cancer-driving viral oncogene in a lymphopenic host, we created an ideal situation of T_E cell therapy, which, however, at least partially can be extrapolated into the clinic. In our model, T_E cells recognized the target antigen as foreign and were of high avidity, whereas in the current clinical trials, T_E cells were directed against tumor-associated (self) antigens (TAAs) isolated from the tolerant repertoire, which likely yields predominantly low-avidity T_E cells. This may be one reason why tumors escape T_E cell therapy in patients but not in our model. However, the possibility to select high-affinity human T cell receptors (TCRs) against any human TAAs from the nontolerant repertoire (Li et al., 2010) and their use for TCR gene therapy (Schumacher, 2002) might allow engineering of T_E cells in the future for clinical use, which may be as effective as TCR-I T_E cells against Tet-TagLuc tumors. Another reason that T_E cell therapy is so effective in our model may be because we targeted a viral cancer-driving oncogene, which makes immune escape more difficult. Cancer-driving antigens have not been targeted by T_E cell therapy in the clinic, which might be possible with Merkel cell carcinoma, a rare disease caused by an SV40-related polyomavirus containing a homologous Tag (Feng et al., 2008). Currently, it is unknown whether the T_E cell therapy of fibrosarcoma and gastric carcinoma, albeit employed with large established tumors, is similarly effective in models of primary (nontransplanted) tumors. It also needs to be seen whether and under which conditions TAAs, whose expression is often not necessary for a malignant phenotype, can be targeted with similar efficacy in the clinic by T_E cells as shown here for TagLuc. In conclusion, adoptive T cell therapy and drug-based cancer treatment were both highly effective in mouse models of fibrosarcoma and gastric carcinoma, but only T cells killed cancer cells and simultaneously destroyed the tumor vasculature, which may be critical to prevent escape.

EXPERIMENTAL PROCEDURES

Mice

Rag-1$^{-/-}$ or *Rag-2*$^{-/-}$ (*Rag*$^{-/-}$) mice and *TCR-I* mice, which are transgenic for an H-2-D^b-restricted Tag epitope I-specific (Vβ7$^+$) T cell receptor (Staveley-O'Carroll et al., 2003), were obtained from The Jackson Laboratory. *Rag*$^{-/-}$/*OT-1* and CB17/Icr*Prkdc*^{scid}/IcrlcoCrl (*SCID*) mice were obtained from Taconic and Charles River, respectively. *LoxP-Tag* × *Alb-Cre* mice have been described elsewhere (Willimsky et al., 2008). As skin graft donors, *rtTA-CM2* transgenic mice expressing the reverse transactivator *rtTA2*^{S}*-M2* and *CAG-Fluc* mice expressing the firefly luciferase (*Fluc*), both controlled by the *CAG* promoter, on an albino B6 genetic background (unpublished data) were used. Generation of *TRE*^{loxP}*stop*^{loxP}*TagLuc* transgenic mice is described in Supplemental Experimental Procedures. These mice express a dox-inducible TagLuc fusion gene (Buschow et al., 2010), which is separated from the TRE promoter by a loxP site-flanked stop cassette. All animal experiments were conducted in accordance with institutional and national guidelines and regulations, after approval by the Landesamt für Gesundheit und Soziales (Berlin).

Cancer Cell Lines

Cells were cultured in Dulbecco's modified eagle medium (GIBCO), supplemented with 10% heat-inactivated fetal calf serum (PAN, Biotech) and 50 μg/ml gentamicin (GIBCO). Tet-TagLuc cells were derived from tail fibroblasts of a *TRE^{loxP}stop^{loxP}TagLuc* heterozygous mouse. Fibroblasts were isolated by collagenase digestion (type II, Invitrogen) and after three culture passages were infected with adenoviruses and retroviruses, encoding the *Cre* recombinase (Willimsky and Blankenstein, 2005) and the Tet-off transactivator (*tTA*, Clontech, #631003), respectively. Cells at passage 19 were injected subcutaneously (s.c.) into a *Rag*$^{-/-}$ mouse, and a cell line was established from the resulting tumor. MCA205 fibrosarcoma cells were cotransfected with pCAG-TagLuc (Buschow et al., 2010) and pMSCVpuro (Clontech) plasmid DNA (ratio 10:1) with lipofectamine 2000 reagent (Invitrogen), selected for puromycin (Sigma) resistance (10 μg/ml), and TagLuc-expressing clones were identified by Fluc activity. A cell line (TC200) of a gastric carcinoma, grown in a *TRE^{loxP}stop^{loxP}TagLuc* × *rtTA-CM2* mouse, was established and passaged once in a *Rag*$^{-/-}$ mouse (TC200.09). J558-IFNγ^{IND} cancer cells were described previously (Briesemeister et al., 2011). Between 1 and 5 × 10^6 tumor cells were s.c. injected into mice as indicated. Tumor growth and regression, respectively, were analyzed by BL imaging and determination of tumor volume by caliper measurement according to the formula (xyz)/2.

Adoptive T Cell Transfer

CD8$^+$ T cells of *TCR-I* mice were isolated by negative magnetic-activated cell sorting (Miltenyi Biotec, #130-090-859) 7 days after immunization with 1 × 10^7 Tag$^+$ 16.113 cells (Willimsky and Blankenstein, 2005) and 1 × 10^6 cells were injected intravenously (i.v.) into mice. T cells were analyzed by flow cytometry with anti-CD8a (RM4-5) and anti-Vβ7 antibodies (BD PharMingen) and peptide I/D^b tetramers (Beckman-Coulter). Alternatively, 1 × 10^7 splenocytes of *LoxP-Tag x Alb-Cre* mice were injected i.v. into *Rag*$^{-/-}$*/OT-1* mice. Blood cells were stained with anti-CD8a and anti-Vβ5 (MR9-4) antibodies and analyzed by flow cytometry.

Doxycycline Treatment

Dox (0.2–1 mg/ml; Sigma) was administered by light-protected drinking water supplemented with 5% sucrose twice a week, or 0.5–1 μg/ml dox was added to the cell culture medium every 2 days.

Bioluminescent Detection

Mice received 3 mg of D-luciferin (Biosynth) i.p., dissolved in PBS (30 mg/ml). After 10 min, mice were anesthetized by Isofluran and imaged. The exposure time for BL image acquisition was 1 s or 60 s, depending on the signal strength. The BL imaging data were analyzed with Living Image software (Caliper Life Science). For in vitro cell culture, 1 × 10^6 cells were seeded in duplicates in 96-well-plates, D-luciferin was added to the cell culture medium (15 μg/ml), and luciferase activity was quantified using a Mithras LB 940 luminometer (Berthold Technologies).

Skin Transplantation

Transplantation of full thickness skin grafts was performed by standard procedure.

IVMPM

Imaging procedures were performed as described previously (Herrmann et al., 2010). Briefly, mice received 100 μg of dextran-rhodamine (Invitrogen) and 10 μg of Annexin V-FITC (BioVision) or 250 μg of Hoechst dye 15 min prior to imaging. Signals of the extracellular matrix are given by second harmonic generation. Fluorescent emission was acquired using an Ultima Multiphoton Microscopy System (Prairie Technologies). T cells were labeled with 5 μM CellTracker Blue CMAC (7-amino-4-chloromethylcoumarin; Invitrogen) before transfer.

SUPPLEMENTAL INFORMATION

Supplemental Information includes four figures and Supplemental Experimental Procedures and can be found with this article online at doi:10.1016/j.ccr.2011.10.019.

ACKNOWLEDGMENTS

We thank Monika Babka, Katrin Hönig, Simone Spieckermann, Markus Hensel, Stephanie Kupsch, and Christel Westen for technical assistance; Ronald Naumann for oocyte injection; Cynthia Perez and Ana Jukica for discussion; and Maja Schreiber for critical reading. This work was supported by grants from the DFG (SFB TR36), the European Community (FP6 grant "ATTACK"), and the "Alliance" program of the HGF (HA-202).

Received: March 2, 2010
Revised: May 23, 2011
Accepted: October 18, 2011
Published: December 12, 2011

REFERENCES

Blankenstein, T. (2005). The role of tumor stroma in the interaction between tumor and immune system. Curr. Opin. Immunol. *17*, 180–186.

Blohm, U., Potthoff, D., van der Kogel, A.J., and Pircher, H. (2006). Solid tumors "melt" from the inside after successful CD8 T cell attack. Eur. J. Immunol. *36*, 468–477.

Briesemeister, D., Sommermeyer, D., Loddenkemper, C., Loew, R., Uckert, W., Blankenstein, T., and Kammertoens, T. (2011). Tumor rejection by local interferon γ induction in established tumors is associated with blood vessel destruction and necrosis. Int. J. Cancer *128*, 371–378.

Buschow, C., Charo, J., Anders, K., Loddenkemper, C., Jukica, A., Alsamah, W., Perez, C., Willimsky, G., and Blankenstein, T. (2010). In vivo imaging of an inducible oncogenic tumor antigen visualizes tumor progression and predicts CTL tolerance. J. Immunol. *184*, 2930–2938.

Casares, N., Pequignot, M.O., Tesniere, A., Ghiringhelli, F., Roux, S., Chaput, N., Schmitt, E., Hamai, A., Hervas-Stubbs, S., Obeid, M., et al. (2005). Caspase-dependent immunogenicity of doxorubicin-induced tumor cell death. J. Exp. Med. *202*, 1691–1701.

Chin, L., Tam, A., Pomerantz, J., Wong, M., Holash, J., Bardeesy, N., Shen, Q., O'Hagan, R., Pantginis, J., Zhou, H., et al. (1999). Essential role for oncogenic Ras in tumour maintenance. Nature *400*, 468–472.

Felsher, D.W., and Bishop, J.M. (1999). Reversible tumorigenesis by MYC in hematopoietic lineages. Mol. Cell *4*, 199–207.

Feng, H., Shuda, M., Chang, Y., and Moore, P.S. (2008). Clonal integration of a polyomavirus in human Merkel cell carcinoma. Science *319*, 1096–1100.

Gooding, L.R. (1982). Characterization of a progressive tumor from C3H fibroblasts transformed in vitro with SV40 virus: immunoresistance in vivo correlates with phenotypic loss of H-2Kk. J. Immunol. *129*, 1306–1312.

Gorre, M.E., Mohammed, M., Ellwood, K., Hsu, N., Paquette, R., Rao, P.N., and Sawyers, C.L. (2001). Clinical resistance to STI-571 cancer therapy caused by BCR-ABL gene mutation or amplification. Science *293*, 876–880.

Gossen, M., and Bujard, H. (2002). Studying gene function in eukaryotes by conditional gene inactivation. Annu. Rev. Genet. *36*, 153–173.

Herrmann, A., Kortylewski, M., Kujawski, M., Zhang, C., Reckamp, K., Armstrong, B., Wang, L., Kowolik, C., Deng, J., Figlin, R., and Yu, H. (2010). Targeting Stat3 in the myeloid compartment drastically improves the in vivo antitumor functions of adoptively transferred T cells. Cancer Res. *70*, 7455–7464.

Hillen, W., and Berens, C. (1994). Mechanisms underlying expression of Tn10 encoded tetracycline resistance. Annu. Rev. Microbiol. *48*, 345–369.

Hinrichs, W., Kisker, C., Düvel, M., Müller, A., Tovar, K., Hillen, W., and Saenger, W. (1994). Structure of the Tet repressor-tetracycline complex and regulation of antibiotic resistance. Science *264*, 418–420.

Huettner, C.S., Zhang, P., Van Etten, R.A., and Tenen, D.G. (2000). Reversibility of acute B-cell leukaemia induced by BCR-ABL1. Nat. Genet. *24*, 57–60.

Jonkers, J., and Berns, A. (2004). Oncogene addiction: sometimes a temporary slavery. Cancer Cell *6*, 535–538.

Kabeya, Y., Mizushima, N., Ueno, T., Yamamoto, A., Kirisako, T., Noda, T., Kominami, E., Ohsumi, Y., and Yoshimori, T. (2000). LC3, a mammalian homologue of yeast Apg8p, is localized in autophagosome membranes after processing. EMBO J. *19*, 5720–5728.

Kast, W.M., Offringa, R., Peters, P.J., Voordouw, A.C., Meloen, R.H., van der Eb, A.J., and Melief, C.J. (1989). Eradication of adenovirus E1-induced tumors by E1A-specific cytotoxic T lymphocytes. Cell *59*, 603–614.

Knight, Z.A., Lin, H., and Shokat, K.M. (2010). Targeting the cancer kinome through polypharmacology. Nat. Rev. Cancer *10*, 130–137.

Kondo, Y., Kanzawa, T., Sawaya, R., and Kondo, S. (2005). The role of autophagy in cancer development and response to therapy. Nat. Rev. Cancer *5*, 726–734.

Kuerbitz, S.J., Plunkett, B.S., Walsh, W.V., and Kastan, M.B. (1992). Wild-type p53 is a cell cycle checkpoint determinant following irradiation. Proc. Natl. Acad. Sci. USA *89*, 7491–7495.

Kumar, V., Fausto, N., and Abbas, A. (2004). Neoplasia, Seventh Edition (Philadelphia: W.B. Saunders/Elsevier).

Li, L.-P., Lampert, J.C., Chen, X., Leitao, C., Popović, J., Müller, W., and Blankenstein, T. (2010). Transgenic mice with a diverse human T cell antigen receptor repertoire. Nat. Med. *16*, 1029–1034.

Liu, J.Q., and Bai, X.F. (2008). Overcoming immune evasion in T cell therapy of cancer: lessons from animal models. Curr. Mol. Med. *8*, 68–75.

Moody, S.E., Sarkisian, C.J., Hahn, K.T., Gunther, E.J., Pickup, S., Dugan, K.D., Innocent, N., Cardiff, R.D., Schnall, M.D., and Chodosh, L.A. (2002). Conditional activation of Neu in the mammary epithelium of transgenic mice results in reversible pulmonary metastasis. Cancer Cell *2*, 451–461.

Mylin, L.M., Schell, T.D., Epler, M., Kusuma, C., Assis, D., Matsko, C., Smith, A., Allebach, A., and Tevethia, S.S. (2007). Diversity of escape variant mutations in Simian virus 40 large tumor antigen (SV40 Tag) epitopes selected by cytotoxic T lymphocyte (CTL) clones. Virology *364*, 155–168.

Pao, W., Miller, V.A., Politi, K.A., Riely, G.J., Somwar, R., Zakowski, M.F., Kris, M.G., and Varmus, H. (2005). Acquired resistance of lung adenocarcinomas to gefitinib or erlotinib is associated with a second mutation in the EGFR kinase domain. PLoS Med. *2*, e73.

Qin, Z., and Blankenstein, T. (2000). CD4+ T cell-mediated tumor rejection involves inhibition of angiogenesis that is dependent on IFN γ receptor expression by nonhematopoietic cells. Immunity *12*, 677–686.

Qin, Z., Schwartzkopff, J., Pradera, F., Kammertoens, T., Seliger, B., Pircher, H., and Blankenstein, T. (2003). A critical requirement of interferon γ-mediated angiostasis for tumor rejection by CD8+ T cells. Cancer Res. *63*, 4095–4100.

Rakhra, K., Bachireddy, P., Zabuawala, T., Zeiser, R., Xu, L., Kopelman, A., Fan, A.C., Yang, Q., Braunstein, L., Crosby, E., et al. (2010). CD4(+) T cells contribute to the remodeling of the microenvironment required for sustained tumor regression upon oncogene inactivation. Cancer Cell *18*, 485–498.

Restifo, N.P., Marincola, F.M., Kawakami, Y., Taubenberger, J., Yannelli, J.R., and Rosenberg, S.A. (1996). Loss of functional beta 2-microglobulin in metastatic melanomas from five patients receiving immunotherapy. J. Natl. Cancer Inst. *88*, 100–108.

Schreiber, K., Rowley, D.A., Riethmüller, G., and Schreiber, H. (2006). Cancer immunotherapy and preclinical studies: why we are not wasting our time with animal experiments. Hematol. Oncol. Clin. North Am. *20*, 567–584.

Schüler, T., and Blankenstein, T. (2003). Cutting edge: CD8+ effector T cells reject tumors by direct antigen recognition but indirect action on host cells. J. Immunol. *170*, 4427–4431.

Schumacher, T.N. (2002). T-cell-receptor gene therapy. Nat. Rev. Immunol. *2*, 512–519.

Skipper, H.E. (1965). The effects of chemotherapy on the kinetics of leukemic cell behavior. Cancer Res. *25*, 1544–1550.

Spiotto, M.T., Rowley, D.A., and Schreiber, H. (2004). Bystander elimination of antigen loss variants in established tumors. Nat. Med. *10*, 294–298.

Staveley-O'Carroll, K., Schell, T.D., Jimenez, M., Mylin, L.M., Tevethia, M.J., Schoenberger, S.P., and Tevethia, S.S. (2003). In vivo ligation of CD40 enhances priming against the endogenous tumor antigen and promotes CD8+ T cell effector function in SV40 T antigen transgenic mice. J. Immunol. *171*, 697–707.

Stoler, D.L., Chen, N., Basik, M., Kahlenberg, M.S., Rodriguez-Bigas, M.A., Petrelli, N.J., and Anderson, G.R. (1999). The onset and extent of genomic instability in sporadic colorectal tumor progression. Proc. Natl. Acad. Sci. USA *96*, 15121–15126.

Tang, Y., Kim, M., Carrasco, D., Kung, A.L., Chin, L., and Weissleder, R. (2005). In vivo assessment of RAS-dependent maintenance of tumor angiogenesis by real-time magnetic resonance imaging. Cancer Res. *65*, 8324–8330.

Uckert, W., Kammertöns, T., Haack, K., Qin, Z., Gebert, J., Schendel, D.J., and Blankenstein, T. (1998). Double suicide gene (cytosine deaminase and herpes simplex virus thymidine kinase) but not single gene transfer allows reliable elimination of tumor cells in vivo. Hum. Gene Ther. *9*, 855–865.

Weinstein, I.B. (2002). Cancer: addiction to oncogenes—the Achilles heal of cancer. Science *297*, 63–64.

Willimsky, G., and Blankenstein, T. (2005). Sporadic immunogenic tumours avoid destruction by inducing T-cell tolerance. Nature *437*, 141–146.

Willimsky, G., Czéh, M., Loddenkemper, C., Gellermann, J., Schmidt, K., Wust, P., Stein, H., and Blankenstein, T. (2008). Immunogenicity of premalignant lesions is the primary cause of general cytotoxic T lymphocyte unresponsiveness. J. Exp. Med. *205*, 1687–1700.

Yee, C., Thompson, J.A., Roche, P., Byrd, D.R., Lee, P.P., Piepkorn, M., Kenyon, K., Davis, M.M., Riddell, S.R., and Greenberg, P.D. (2000). Melanocyte destruction after antigen-specific immunotherapy of melanoma: direct evidence of t cell-mediated vitiligo. J. Exp. Med. *192*, 1637–1644.

Ying, L., Lau, A., Alvira, C.M., West, R., Cann, G.M., Zhou, B., Kinnear, C., Jan, E., Sarnow, P., Van de Rijn, M., and Rabinovitch, M. (2009). LC3-mediated fibronectin mRNA translation induces fibrosarcoma growth by increasing connective tissue growth factor. J. Cell Sci. *122*, 1441–1451.

Zhang, B., Karrison, T., Rowley, D.A., and Schreiber, H. (2008). IFN-γ- and TNF-dependent bystander eradication of antigen-loss variants in established mouse cancers. J. Clin. Invest. *118*, 1398–1404.